Molecular Biology of the Cell
Vol. 18, 47–56, January 2007

Rab8-dependent Recycling Promotes Endosomal Cholesterol Removal in Normal and Sphingolipidosis Cells

Matts D. Linder,* Riikka-Liisa Uronen,* Maarit Hölttä-Vuori,* Peter van der Sluijs,† Johan Peränen,‡ and Elina Ikonen*

*Institute of Biomedicine/Anatomy and ‡Institute of Biotechnology, University of Helsinki, FI-00014 Helsinki, Finland; and †Department of Cell Biology, University Medical Center Utrecht, 3584 CX Utrecht, The Netherlands

Submitted July 3, 2006; Revised September 13, 2006; Accepted October 10, 2006

The mechanisms by which low-density lipoprotein (LDL)-cholesterol exits the endocytic circuits are not well understood. The process is defective in Niemann–Pick type C (NPC) disease in which cholesterol and sphingolipids accumulate in late endosomal compartments. This is accompanied by defective cholesterol esterification in the endoplasmic reticulum and impaired ATP-binding cassette transporter A1 (ABCA1)-dependent cholesterol efflux. We show here that overexpression of the recycling/exocytic Rab GTPase Rab8 rescued the late endosomal cholesterol deposition and sphingolipid mistrafficking in NPC fibroblasts. Rab8 redistributed cholesterol from late endosomes to the cell periphery and stimulated cholesterol efflux to the ABCA1-ligand apolipoprotein A-I (apoA-I) without increasing cholesterol esterification. Depletion of Rab8 from wild-type fibroblasts resulted in cholesterol deposition within late endosomal compartments. This cholesterol accumulation was accompanied by impaired clearance of LDL-cholesterol from endocytic circuits to apoA-I and could not be bypassed by liver X receptor activation. Our findings establish Rab8 as a key component of the regulatory machinery that leads to ABCA1-dependent removal of cholesterol from endocytic circuits.

INTRODUCTION

Niemann–Pick type C (NPC) disease is one of the classical, monogenic cholesterol accumulation disorders in humans. The cellular pathology has been first characterized roughly 20 years ago (Pentchev *et al*., 1985; Liscum and Faust, 1987), and the disease has since been a subject of intense research efforts. By investigating the molecular basis of NPC pathology, researchers hope to learn more about how cells normally handle cholesterol and about factors predisposing to more common disorders of cholesterol transport and homeostasis. The genes mutated in NPC disease, NPC1 or NPC2, have been characterized previously (Carstea *et al*., 1997; Naureckiene *et al*., 2000). Both are capable of interacting with cholesterol (Okamura *et al*., 1999; Ohgami *et al*., 2004), but their precise functions are unknown.

NPC cells exhibit a defect in the intracellular trafficking of low-density lipoprotein (LDL)-derived cholesterol. In NPC cells, LDL is taken up by receptor-mediated endocytosis, and the LDL cholesteryl esters are hydrolyzed to free cholesterol and fatty acid by lysosomal acid lipase. However, cholesterol is not capable of efficiently exiting the hydrolytic compartments and accumulates therein (Pentchev *et al*., 1994). Cholesterol has impaired access to the endoplasmic reticulum for reesterification and for regulation of the transcriptional apparatus of lipid balance. Therefore, cholesterol biosynthesis and LDL receptor levels are maintained at inappropriately high levels. Moreover, the generation of oxysterols is impaired in NPC cells. This results in decreased activation of the nuclear hormone receptor liver X receptor (LXR) and impaired cholesterol efflux via the LXR-regulated cholesterol transporter ATP-binding cassette transporter A1 (ABCA1) (Choi *et al*., 2003; Frolov *et al*., 2003).

In addition to cholesterol, other lipids, in particular sphingolipids, accumulate in the late endocytic organelles of NPC cells. One of the prevailing ideas is that, whatever the basic mechanism, the NPC cell pathology presents itself as an endosomal traffic jam (Liscum, 2000; Simons and Gruenberg, 2000). The largest subfamily of Ras GTPases, Rab proteins, governs key processes that provide compartmental specificity for membrane traffic (Zerial and McBride, 2001). Rab-dependent membrane transport apparently represents one of the systems clearing cholesterol from late endocytic organelles. This was suggested by the inhibition of late endosomal cholesterol removal by Rab-guanine nucleotide dissociation inhibitor (GDI) (Holtta-Vuori *et al*., 2000). Moreover, overexpression of late endosomal Rab proteins rescued the cholesterol and sphingolipid accumulation in NPC cells. Rab9 overexpression was found to complement the NPC phenotype in two independent studies, and Rab7 overexpression was reported to act similarly in one study but not in another (Choudhury *et al*., 2002; Walter *et al*., 2003). Rab proteins move between the target membrane and the cytoplasm during their activity cycle. Membrane cholesterol loading impairs the extractability of several Rabs, including Rab4, Rab5, Rab7, and Rab9, from membranes by GDI (Lebrand *et al*., 2002; Choudhury *et al*., 2004; Ganley and

This article was published online ahead of print in *MBC in Press* (http://www.molbiolcell.org/cgi/doi/10.1091/mbc.E06–07–0575) on October 18, 2006.

Address correspondence to: Elina Ikonen (elina.ikonen@helsinki.fi).

Abbreviations used: ABCA1, ATP-binding cassette transporter A1; apoA-I, apolipoprotein A-I; CTxB, cholera toxin subunit B; ER, endoplasmic reticulum; GDI, GDP dissociation inhibitor; GFP, green fluorescent protein; Lamp1, lysosome-associated membrane protein 1; LDL, low-density lipoprotein; LXR, liver X receptor; NPC, Niemann–Pick disease type C; RNAi, RNA interference; SFV, Semliki Forest virus; shRNA, short hairpin RNA.

Pfeffer, 2006). Thus, sequestration of Rab proteins in membranes may contribute to the cellular pathology of NPC disease.

We have recently shown that LXR activation enhances cholesterol trafficking to the plasma membrane, where it becomes available for efflux, at the expense of esterification (Rigamonti *et al*., 2005). However, no Rab proteins have so far been identified as regulators of ABCA1-dependent cholesterol efflux. In this study, we investigated the involvement of Rab8 that has previously been implicated in exocytic/recycling membrane trafficking, in cholesterol removal from the endocytic circuits. Rab8 localizes to the Golgi region, vesicular structures, and peripheral membrane ruffles (Chen *et al*., 1993; Huber *et al*., 1993b) and has been implicated in polarized membrane traffic to the cell surface (Huber *et al*., 1993a,b; Deretic *et al*., 1995; Peranen *et al*., 1996; Hattula *et al*., 2002), possibly involving the recycling endosomes as an intermediate (Ang *et al*., 2004). We used the previously described NPC complementation strategy as a starting point in the present study. Our results provide the first evidence for Rab8 as a regulator of intracellular cholesterol transport. More specifically, data from both Rab8-overexpressing NPC cells and Rab8-depleted normal cells indicate a role for Rab8 in the mobilization of cholesterol from endocytic circuits to the ABCA1-ligand apolipoprotein A-I (apoA-I). Importantly, the beneficial effects of elevated Rab8 levels in cholesterol-loaded cells are not explainable solely by an increased pool of GDI-extractable Rab, because Rab8 membrane extractability was not compromised in NPC cells.

MATERIALS AND METHODS

Materials

Cell culture media, defatted bovine serum albumin (BSA), ATP, GDP, chymostatin, leupeptin, antipain, pepstatin, T0901317, and filipin were from Sigma-Aldrich (St. Louis, MO). Radiolabeled lipids were from GE Healthcare (Little Chalfont, Buckinghamshire, United Kingdom) and apoA-I from the Swiss Red Cross (Geneva, Switzerland). Alexa488- or 568-conjugated secondary antibodies and Alexa594-conjugated cholera toxin subunit B (CTxB) were from Invitrogen (Carlsbad, CA). Anti-Rab8 and anti-GM130 monoclonal antibodies were from BD Biosciences (San Jose, CA). Anti-Rab8 rabbit polyclonal antibodies have been described previously (Peranen *et al*., 1996). Anti-Rab7 antibody was a kind gift from Philippe Chavrier (Membrane and Cytoskeleton Dynamics Group, CNRS/Institut Curie, Paris, France). Anti-Lamp1 antibodies (H4A3) were from Developmental Studies Hybridoma Bank (University of Iowa, Iowa City, IA). 92-99 control fibroblasts and F92-116 NPC1 patient fibroblasts have been described previously (Holtta-Vuori *et al*., 2000; Blom *et al*., 2003). GM3123 NPC1 patient fibroblasts were from Coriell Cell Repositories (Camden, NJ). Fibroblasts were cultured as described previously (Blom *et al*., 2003). Peritoneal macrophages were isolated from wild-type BALB/c mice and cultured in DMEM/10% fetal bovine serum (FBS), 10 mM HEPES, pH 7.4, 100 IU/ml penicillin, and 100 μg/ml streptomycin. Acetyl-LDL loading was carried out at 100 μg protein/ml for 18 h.

Plasmid Constructs and Cell Transfection

pEGFP and pEYFP were from Clontech (Mountain View, CA). Rab7-pEGFP and Rab4-pEGFP have been described previously (Bielli *et al*., 2001; Holtta-Vuori *et al*., 2002). The rab4aDCGC-pEYFP (Rab4Δ) construct was created by subcloning the insert from rab4aCT3-pFRSV lacking the cys-gly-cys prenylation motif (van der Sluijs *et al*., 1992) into the EcoRI site of the pEYFP-C3 vector. Rab8-pEGFP has been described previously (Hattula and Peranen, 2000). Cells were transfected with FuGENE6 (Roche Diagnostics, Mannheim, Germany) according to manufacturer's instructions and analyzed at 48 h posttransfection unless otherwise indicated.

RNA Interference

The target sequence for knockdown of Rab8 has been described previously (Schuck *et al*., 2004). The psiSTRIKE hMGFP (Promega, Madison, WI) was used as template to introduce Rab8-specific and scrambled short hairpin RNA (shRNA) sequences into the vector by inverse polymerase chain reaction (PCR) as detailed by the manufacturer, by using the following primers: Rab8-forward, 5′-CGTTCCTTGGAAACTTGTCTTTTTCTGCAGGAGACGAGATCTCCCTCC-3′; Rab8-inverse, 5′-TGACAGGAAGCGTTCCTTGGAAACTTGTCGGTGTTTCGTCCTTTCCACAAGATA-3′; scramble-forward, 5′-ACTGTCTGTCAGCTAGTTCTTTTTGTGCAGGAGACGAGATCTCCGAGCTCC 3-′; and scramble-inverse, 5′TGACAGGAAGACTGTCTGTCAGCTAGTTCGGTGTTTCGTCCTTTCCACAAGATA-3′. The sequences of the hairpin regions of the plasmids (pRab8-shRNA and pScramble-shRNA) were verified by sequencing. Fibroblasts were transfected with shRNA plasmids using FuGENE6 and incubated as indicated in the individual experiments.

Immunocytochemistry

Cells were fixed with 4% paraformaldehyde for 20 min and quenched with 50 mM NH_4Cl for 10 min. For staining with anti-Rab8 polyclonal antibodies, cells were permeabilized with 0.1% Triton X-100 and blocked with 10% FBS in phosphate-buffered saline (PBS) for 30 min at 37°C. For visualization of free cholesterol, the cells were permeabilized with 0.05% filipin in blocking solution for 30 min at 37°C, followed by incubation with appropriate antibodies before mounting.

Quantification of Filipin Fluorescence

Human skin fibroblasts were transfected with green fluorescent protein (GFP)-tagged Rab proteins for 48 h, fixed, permeabilized with filipin, and stained with anti-lysosome–associated membrane protein (Lamp)1 antibodies and Alexa568-conjugated secondary antibodies. Images of transfected cells were taken in sequence on three channels; GFP, filipin, and Alexa568 on an IX70 inverted microscope (Olympus, Tokyo, Japan) equipped with a Polychrome IV monochromator (TILL Photonics, Gräfelfing, Germany) by using appropriate filters. The filipin fluorescence in GFP-expressing cells was quantified by image processing using Image-Pro software (Media Cybernetics, Silver Spring, MD). The outlines of the cells were drawn manually and after subtraction of coverslip background fluorescence the filipin intensity inside the individual cell boundaries was measured, and regarded as whole cell filipin intensity. For the quantification of filipin fluorescence in Lamp1-positive organelles, the coverslip background and plasma membrane filipin fluorescence were first subtracted. The outlines of Lamp1-positive organelles from the Lamp1 image were determined using software processing and superimposed on the filipin image. The filipin fluorescence inside the area occupied by Lamp1 was subsequently determined.

Labeling of Cells with CTxB

Labeling was carried out essentially as described in Choudhury *et al*. (2002) and Holtta-Vuori *et al*. (2002). Cells were incubated with 2 μg/ml Alexa594-conjugated CTxB in minimal essential medium (MEM) supplemented with 0.35 g/l $NaHCO_3$, 0.01% BSA, 10 mM HEPES, 100 IU/ml penicillin, and 100 μg/ml streptomycin. After incubation at 4°C for 30 min, cells were washed twice with PBS and incubated for 2 h at 37°C in label-free medium before fixation.

Western Blot Analysis

Cells were lysed in 1% Nonidet P-40 in PBS containing protease inhibitors (chymostatin, leupeptin, antipain, and pepstatin at 25 μg/ml each). Protein amounts were assayed according to Lowry *et al*. (1951). Equal amounts of protein (15 μg) were subjected to SDS-PAGE and analyzed by Western blotting as described in Holtta-Vuori *et al*. (2002).

Rab-GDI Extraction

F92-99 or F92-116 fibroblasts were suspended in PBS, containing protease inhibitors (as described above). The cell suspension was passed through a 25-gauge syringe 100 times to break the cells. Nuclei were pelleted by centrifugation at 1000 $\times$ *g* for 10 min at 4°C. Equal amounts (100 μg of protein) of postnuclear supernatant was centrifuged in a Beckman tabletop ultracentrifuge at 100,000 $\times$ *g* for 60 min to pellet the cellular membranes. His_6-tagged Rab-GDI has been described previously (Holtta-Vuori *et al*., 2000). The Rab-GDI extraction of membranes was carried out as described in Cavalli *et al*. (2001) and Choudhury *et al*. (2004). Briefly, the pellet was dissolved in 30 mM HEPES, 75 mM potassium acetate, and 5 mM $MgCl_2$ containing 100 μM ATP and 500 μM GDP and incubated for 20 min at 30°C with varying amounts of Rab-GDI, after which membranes were pelleted by centrifugation at 100,000 $\times$ *g* for 60 min. The pellet was dissolved in SDS-PAGE sample buffer, and proteins were separated by 15% SDS-PAGE followed by Western blotting. The amount of Rab protein remaining in the membranes after the GDI extraction was assessed by incubation with monoclonal anti-Rab8 antibodies followed by enhanced chemiluminescence, and the filters were then stripped and reprobed with anti-Rab7 antibodies.

Recombinant Semliki Forest Viruses (SFVs)

pRab8-SFV (Peranen *et al*., 1996), pLacZ-SFV, and pSFV-Helper constructs were linearized with SpeI, and runoff transcription was performed according to Liljestrom and Garoff (1991). The Rab8 and LacZ transcription mixes were cotransfected with Helper transcription mix to baby hamster kidney cells by using electroporation as described previously (Olkkonen *et al*., 1993). The culture medium was collected after 24 h posttransfection. Titration of virus stocks was performed as described previously (Olkkonen *et al*., 1993).

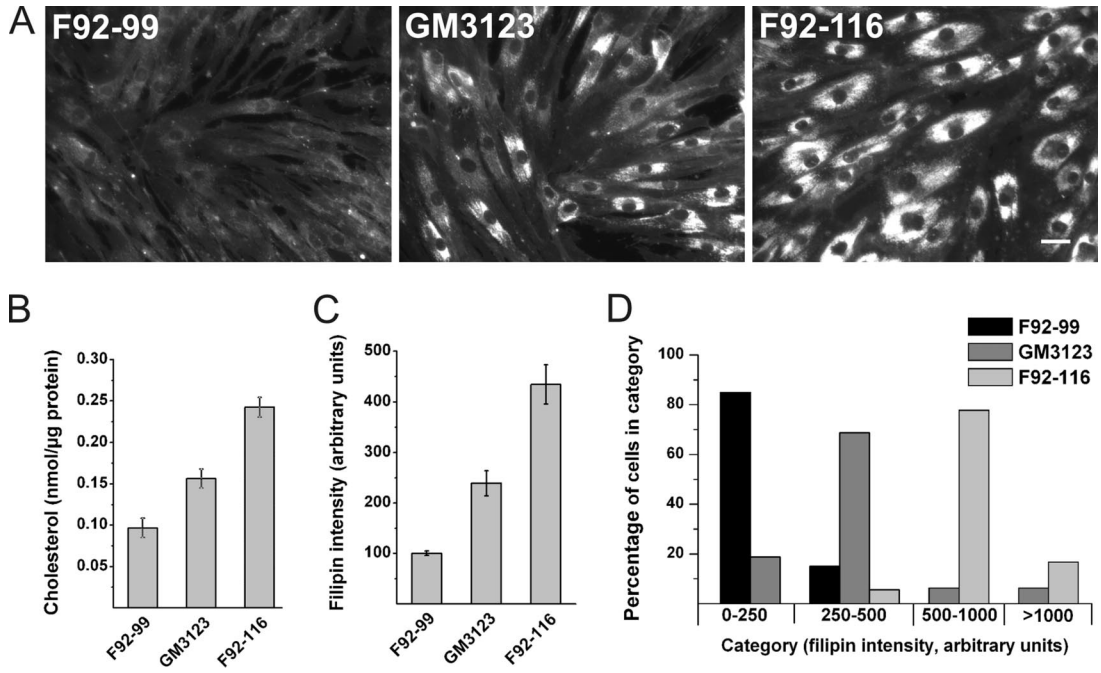

Figure 1. Characterization of human NPC1 fibroblast lines used in the study. (A) Filipin staining of control (F92-99) and two NPC1 patient fibroblast lines (GM3123 and F92-116). (B) Free cholesterol levels were measured biochemically (n = 6 from two independent samples for each cell line). (C) Intensity of filipin staining in a cell population (n = 40). (D) Individual cells grouped into categories based on filipin staining intensity. Bar, 40 μm.

Measurement of Cholesterol Esterification

Cells were seeded on 3.5-cm dishes and incubated in Earle's (E)-MEM supplemented with 10% lipoprotein-deficient serum (LPDS) prepared as described in Goldstein *et al*. (1983), 2 mM L-glutamine, 100 IU/ml penicillin, 100 μg/ml streptomycin, and 10 mM HEPES, pH 7.4, for 24 h. Cells were then infected with either Rab8/SFV or LacZ/SFV for 1 h after which the medium was changed to fresh 10% LPDS medium and incubated for 18 h. The cells were washed twice with PBS and incubated in E-MEM supplemented with 2% defatted BSA, [^{3}H]oleic acid (5 μCi/ml) and 50 μg/ml LDL for 6 h after which the cells were harvested. Lipids were extracted and cholesterol esterification measured as described previously (Holtta-Vuori *et al*., 2002).

Cholesterol Efflux

Cells were seeded on 24-well plates and incubated in the presence of [^{3}H]cholesterol (1 μCi/ml) for 24 h. Cells were then infected with either Rab8/SFV or LacZ/SFV for 1 h after which the medium was replaced with complete medium supplemented with [^{3}H]cholesterol and incubated for 6 h. Cells were washed three times with PBS and incubated in serum-free medium supplemented with 10 μg/ml apoA-I for 18 h. The medium and cells were collected, and radioactivity was determined by liquid scintillation counting.

Cholesterol Mass Measurements

Control and NPC1 fibroblast cultures were infected with either Rab8/SFV or LacZ/SFV for 1 h after which the medium was replaced with complete medium. After 18 h, the cells were harvested, cell pellets were lysed on ice in 2% NaCl, and aliquots were taken for protein assay. Lipids were extracted (Bligh and Dyer, 1959) from samples adjusted for protein concentration, and the free sterol amount was determined according to Gamble *et al*. (1978). Alternatively, the extracted lipids were applied on HPTLC Silica Gel 60 F_{524} plates (Merck, Darmstadt, Germany) by using an automatic tin layer chromatography (TLC) sampler 4 (Camag, Berlin, Germany). The TLC plates were run using hexane/diethyl ether/acetic acid (80:20:1) as solvent. Lipids were visualized by staining with 3% copper sulfate and 8% phosphorous acid, followed by heating at 180°C for 5 min. The intensity of the bands was quantified using Tina 2.1 software (Raytest, Pittsburgh, PA).

Statistics

Statistical significance was determined using two-tailed Student's *t* test; $p < 0.05$ was considered statistically significant.

RESULTS

Characterization of the Human NPC1 Fibroblast Lines

In this study, two previously characterized NPC primary fibroblast lines with identified NPC1 mutations were used. GM3123 has been used in previous Rab complementation studies (Choudhury *et al*., 2002, 2004; Walter *et al*., 2003), and F92-116 represents a Finnish case of infantile NPC disease (Blom *et al*., 2003). Under normal culture conditions, GM3123 line exhibited a heterogeneous staining pattern with filipin, a fluorescent cholesterol-binding reagent (Figure 1A). Some cells exhibited prominent storage, whereas others seemed virtually indistinguishable from control F92-99 fibroblasts. In the case of F92-116, all of the cells had prominent filipin-positive accumulations and could be readily differentiated from control cells (Figure 1A).

To assess the quantitativeness of filipin staining, we compared the filipin intensities to the actual amounts of unesterified cholesterol in the three cell lines. The results show that filipin intensity shows a good correlation with the sterol amounts in human fibroblasts (Figure 1, B and C). Scoring of the filipin staining intensities in individual cells demonstrated the higher degree of heterogeneity in GM3123 fibroblasts compared with F92-116 cells. A substantial fraction of GM3123 cells overlapped in intensity with control cells, whereas all F92-116 cells exhibited higher intensity (Figure 1D).

Cholesterol Reduction in NPC Fibroblasts upon Overexpression of Rab4, Rab7, or Rab8

Overexpression of GFP fusions of Rab7 or Rab9 have been reported to reduce filipin intensity in the NPC fibroblast line GM3123 (Choudhury *et al*., 2002). To analyze the specificity of Rab-GFP complementation, we studied whether a fluorescent protein alone or fused to a nonprenylated cytosolic mutant Rab (Rab4del, lacking the C-terminal Cys-Gly-Cys

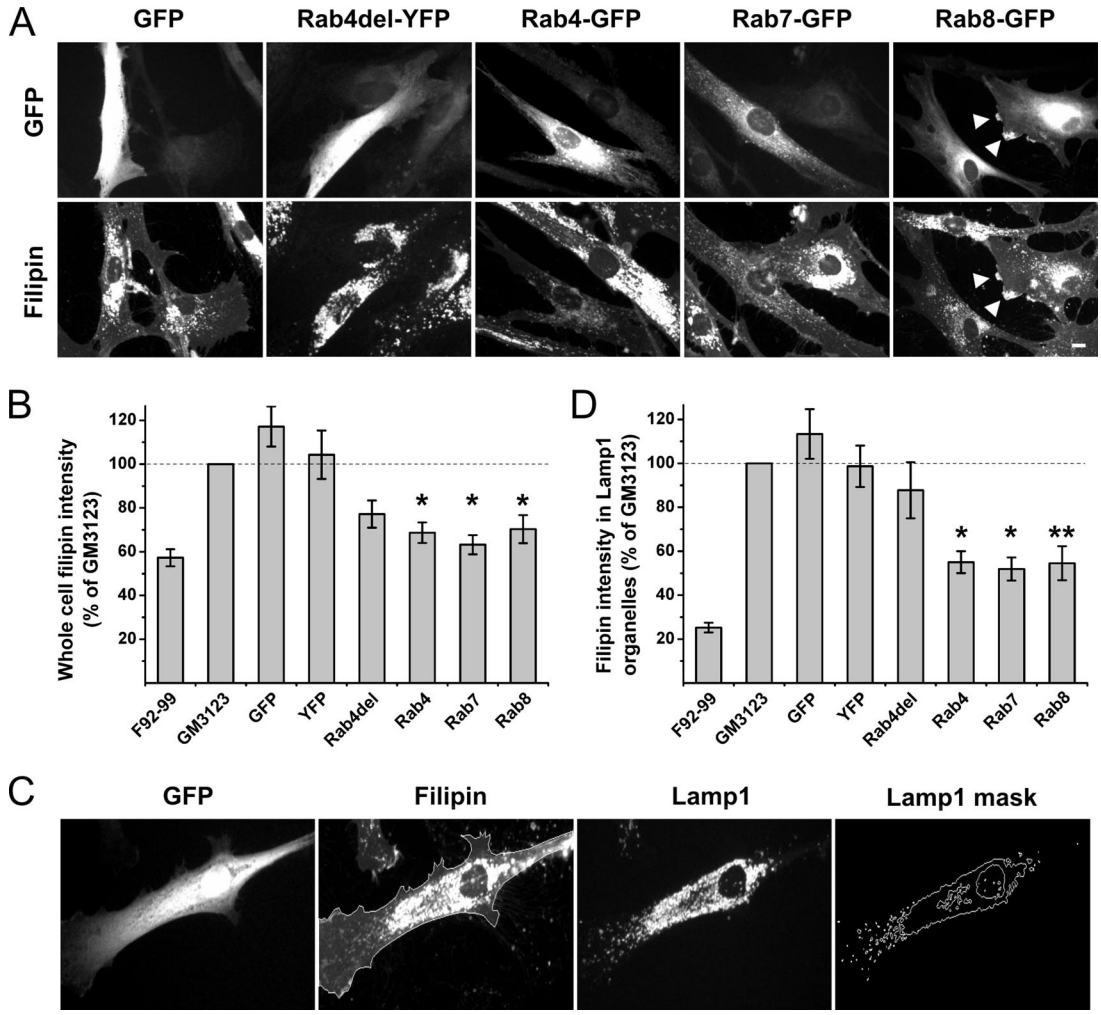

Figure 2. Reduction of cholesterol storage in NPC1 fibroblasts upon overexpression of early, recycling, or late endosomal Rab proteins. (A) GM3123 NPC1 fibroblasts were transfected with fluorescently tagged constructs as indicated. Arrowheads point to filipin and Rab8-GFP–positive structures at the cell periphery. (B) Filipin intensity of untransfected (GM3123) and transfected cells from the same coverslips were quantified; soluble GFP (n = 51), soluble YFP (n = 31), Rab4del-YFP (n = 46), Rab4-GFP (n = 51), Rab7-GFP (n = 79), and Rab8-GFP (n = 32). The values were adjusted in relation to the untransfected cells in the coverslip. Filipin intensity in control F92-99 fibroblasts is shown for reference. (C) The cells were also scored for filipin intensity in Lamp1-positive organelles (see text for details). (D) Quantification of filipin fluorescence in Lamp1 containing organelles (n values same as in B, except for Rab7-GFP, n = 53). Values are mean ± SEM, *$p < 0.05$, **$p \leq 0.01$. Bar, 10 μm.

prenylation motif) affects filipin intensity in these cells. GFP or yellow fluorescent protein (YFP) overexpression alone did not decrease filipin intensity (Figure 2, A and B), but expression of the nonfunctional Rab4 mutant moderately reduced total cellular filipin intensity (Figure 2B). However, considering the substantial heterogeneity in the filipin intensity of unmanipulated GM3123 cells, we wondered whether this could reflect the better transfection efficiency of cells with less storage. Furthermore, the redistribution of filipin to the storage organelles could be appreciated in most GM3123 cells (Figure 1A), and in Rab4del-expressing cells, the labeling of the storage organelles seemed not to be decreased (Figure 2A). We therefore set up a system to monitor the filipin intensity of Lysosome associated membrane protein 1 (Lamp1)-positive organelles as an alternative method to assess complementation. A mask of Lamp1 immunostaining was pasted on the filipin image, and the filipin intensity under this area quantified (Figure 2C). This strategy yielded a larger initial difference between GM3123 and control F92-99 cells (Figure 2D), evidently because of the sequestration of filipin positive material in late endocytic organelles in the disease cells.

Using this more precise method for cholesterol measurement in the late endosomal/lysosomal system, we found that the filipin intensity in Lamp1-positive organelles was not affected by overexpression of GFP, YFP, or the nonprenylated Rab4 mutant (Figure 2D). In contrast, overexpression of the early endosomal wild-type Rab4 or the late endosomal Rab7 significantly decreased filipin intensity in Lamp1-positive organelles (Figure 2, A and D). Using the same strategy, we found that overexpression of Rab8 also efficiently reduced cholesterol deposition in GM3123 cells (Figure 2, A, B, and D). No relationship was observed between the degree of Rab overexpression as detected by GFP fluorescence intensity and the degree of reduction in filipin intensity (data not shown).

We next analyzed whether Rab8 overexpression would also lower cholesterol in the more aggressive accumulation

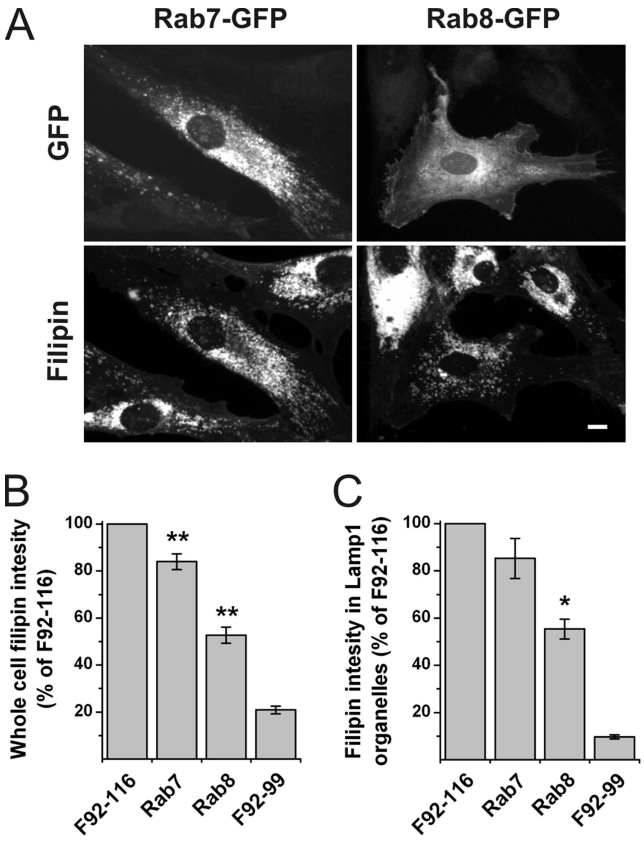

Figure 3. Rab8 effectively reduces cholesterol storage in NPC1 cells with severe lipid deposition. (A) F92-116 NPC1 fibroblasts were transfected with Rab8-GFP or Rab7-GFP. (B) Filipin intensity in whole cells was quantified as in Figure 2B; Rab7-GFP (n = 73), Rab8-GFP (n = 56). (C) Filipin intensity in Lamp1-positive organelles was assayed as in Figure 2D; Rab7-GFP (n = 53), Rab8-GFP (n = 21). Values are mean ± SEM, *$p < 0.05$, **$p \leq 0.01$. Bar, 10 μm.

characteristic to F92-116 NPC fibroblasts. In these NPC fibroblasts, Rab7 overexpression resulted in a small decrease of filipin intensity in whole cells but failed to reduce the filipin intensity in Lamp1-positive organelles (Figure 3, A–C). In contrast, Rab8 overexpression produced a clear reduction in cholesterol storage as measured by the same parameters (Figure 3, A–C).

Rab8 Overexpression Rescues Sphingolipid Transport in NPC Cells

To assess the extent of sphingolipid mistrafficking in NPC cells, we analyzed the cellular itinerary of cholera toxin subunit B (CTxB). CTxB binds to GM1 ganglioside and is known to be transported from the plasma membrane to the Golgi complex in normal cells but in NPC cells, the toxin is mislocalized to endocytic organelles (Sugimoto *et al*., 2001; Choudhury *et al*., 2002) (compare Figure 4A with B). To assess the effect of Rab8 overexpression on GM1 trafficking in NPC cells, CTxB transport was analyzed in GFP- versus Rab8-GFP–expressing GM3123 cells. The toxin was bound on ice for 30 min and chased for 2 h at 37°C. In most GFP-expressing cells, a punctate endosomal staining pattern was observed (Figure 4B), with only 20% of cells exhibiting a predominant Golgi-like localization (Figure 4C). However, in Rab8-GFP–overexpressing cells, CTxB was typically found in the perinuclear area where it colocalized with Rab8 tubular profiles and the Golgi marker GM130 (Figure 4B). The fraction of cells showing a Golgi-like staining pattern of the toxin increased to ~50% in Rab8-overexpressing cells (Figure 4C). We conclude that Rab8 overexpression partially rescued the GM1 transport defect in NPC cells.

Overexpression of Rab8 Redistributes Cholesterol to Peripheral Processes and Increases Cholesterol Efflux from NPC Cells to apoA-I

In addition to an overall decrease in filipin intensity, we noticed that some Rab8-overexpressing cells exhibited a redistribution of filipin labeling to peripheral, Rab8-positive cell protrusions (Figure 2A). Such prominent filipin positive peripheral elements were not present in untransfected cells or in cells expressing other Rab proteins. We found that 14% of Rab8-GFP–overexpressing cells exhibited prominent filipin labeling of peripheral cell processes versus 4% of GFP- and 0% of nonoverexpressing cells (blind quantification of 94 Rab8-GFP, 53 GFP-expressing, and 46 nonoverexpressing cells). This suggests that in Rab8 overexpressing cells a fraction of cholesterol, possibly deriving from the Lamp-positive organelles that became cholesterol de-enriched, was redistributed to the cell periphery.

To analyze biochemical effects of Rab8 overexpression on cholesterol transport, Rab8 was expressed in fibroblasts by using a recombinant SFV. This resulted in the majority of the cells being infected and a robust overexpression of Rab8 (Figure 5A). Moreover, filipin intensity in Lamp1-positive organelles was reduced similarly as upon Rab8 transient

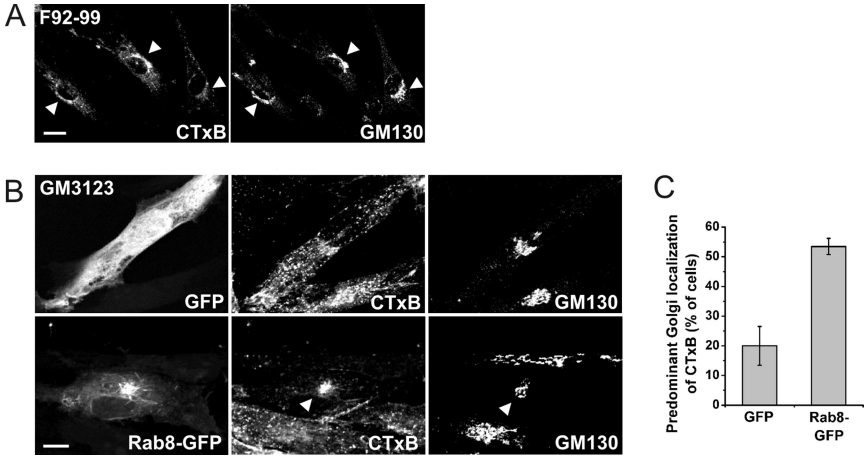

Figure 4. Correction of defective glycolipid trafficking in NPC1 cells upon Rab8 overexpression. (A) Labeling of control F92-99 fibroblasts with CTxB results in a Golgi-like staining pattern that colocalizes with the Golgi marker GM130 (arrowheads). (B) Labeling of NPC1 GM3123 fibroblasts with CTxB shows a punctate staining pattern. Transfection of GM3123 cells with Rab8-GFP increases the Golgi localization of CTxB (arrowheads). (C) The percentage of cells showing a predominant Golgi-like localization of CTxB was scored in Rab8-GFP and GFP transfected cells (n = 126 for GFP and n = 107 for Rab8-GFP, from two independent experiments, mean ± SD). Bars, 20 μm (A) and 10 μm (B).

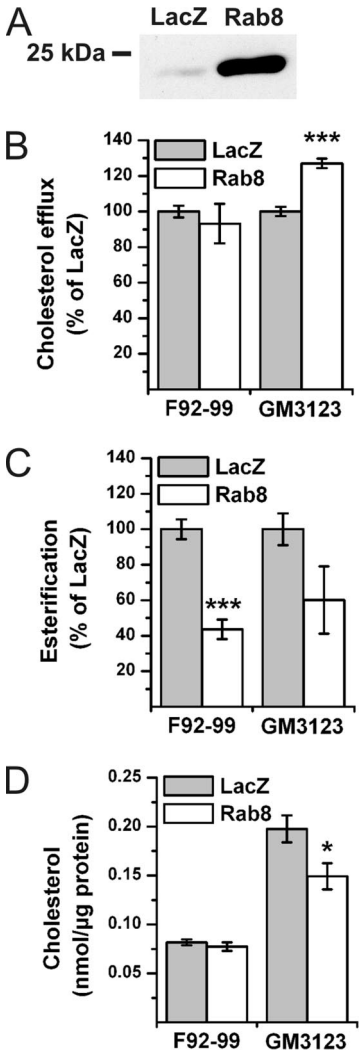

Figure 5. Rab8 increases cholesterol efflux, decreases cholesterol esterification, and decreases cholesterol mass. The effect of Rab8 on cholesterol homeostasis was assessed biochemically by infection of F92-99 control cells and GM3123 NPC1 cells with LacZ/SFV or Rab8/SFV. (A) Anti-Rab8 Western blot from 20 μg of GM3123 cell lysate from recombinant SFV-expressing cells. (B) Cholesterol efflux to apoA-I from Rab8/SFV-infected cells normalized to LacZ/SFV. Cholesterol efflux in LacZ/SFV-infected GM3123 cells was 52.3 $\pm$ 5.43% of that in LacZ/SFV-infected F92-99 cells (mean $\pm$ SEM, n = 5). (C) Rate of cholesterol esterification in recombinant SFV-infected cells. Cholesterol esterification in LacZ/SFV infected GM3123 cells was 17.8 $\pm$ 4.33% of that in LacZ/SFV-infected F92-99 cells (mean $\pm$ SEM, n = 5). (D) Unesterified cholesterol levels in recombinant SFV-expressing cells (mean $\pm$ SEM, n = 5 for GM3123 and n = 3 for F92-99 cells). *$p < 0.05$, ***$p \leq 0.001$.

transfection (data not shown). To measure cholesterol efflux, the cells were radiolabeled with [^{3}H]cholesterol for 18 h before viral infection, infected for 1 h followed by 6 h of chase, and further incubated with apoA-I for 18 h. We found that in NPC fibroblasts Rab8 overexpression resulted in a significant increase in the efflux of cholesterol to apoA-I compared with the LacZ control virus (Figure 5B). No effect on cholesterol efflux was observed in control fibroblasts (Figure 5B). Cholesterol esterification was measured by incorporation of [^{3}H]oleate into cholesteryl esters in response to LDL loading, as in the diagnostics of NPC disease. We found that cholesterol esterification was significantly reduced upon Rab8 overexpression in control fibroblasts, and a similar tendency was observed in NPC fibroblasts (Figure 5C). When the cellular cholesterol amounts were analyzed, we found that the Rab8 overexpression significantly reduced the free cholesterol levels in NPC cells but not in control cells (Figure 5D). In parallel, cholesteryl ester levels did not change (18.8 $\pm$ 0.6% of total sterol in LacZ/SFV versus 17.7 $\pm$ 1.1% in Rab8/SFV-expressing NPC cells [mean $\pm$ SEM; n = 7 measurements]; 20.5 $\pm$ 1.0% of total sterol in LacZ/SFV versus 19.7 $\pm$ 0.3% in Rab8/SFV-expressing control cells [n = 3]). This suggests that the moderate inhibition of esterification was not sufficient to lower the cholesteryl ester levels in NPC cells and that in control cells, cholesterol balance was maintained despite reduced esterification, possibly due to decreased ester hydrolysis.

Rab8 Is Up-Regulated and Its Membrane Extractability Is Not Compromised in Cells with Massive Cholesterol Accumulation

When the endogenous Rab8 expression level was analyzed by Western blotting in F92-116 NPC fibroblasts, Rab8 was found to be up-regulated by ~1.7-fold compared with control fibroblasts (Figure 6, A and B). Moreover, Rab8 was also significantly up-regulated in the cholesterol-filled liver and peritoneal macrophages of the NPC1-deficient mouse as well as upon acetyl-LDL loading of wild-type murine macrophages during foam cell formation (Figure 6, A and B). Because Rab proteins may become sequestered in cholesterol-enriched membranes, we next studied whether the up-regulation of Rab8 in NPC cells was due to this. We analyzed whether the extractability of Rab8 by GDI was compromised in NPC F92-116 fibroblasts and whether the extractability of Rab8 differed from that of Rab7. We found that 1) Rab8 was more easily extracted from membranes by GDI than Rab7 and 2) the extractability of Rab8 was not impaired in NPC cells compared with control cells, under conditions in which a reduction in Rab7 extractability could be demonstrated (Figure 6C). These data strongly suggest that the upregulation of Rab8 upon cholesterol loading is not to counteract the impaired membrane extractability of Rab8 by GDI.

Depletion of Rab8 Results in Late Endosomal Cholesterol Accumulation That Is Refractory to an LXR Agonist Treatment

To address the role of Rab8 in the cholesterol trafficking of normal cells, endogenous Rab8 was depleted using RNA interference (RNAi). The RNAi sequence used reduces Rab8 levels by ~90% in HeLa cells (Hattula and Peränen, unpublished data). Because the transfection frequency of primary fibroblasts is low, we used a plasmid encoding the oligonucleotide hairpin and a GFP reporter. In primary fibroblasts, a clear reduction in Rab8 immunoreactivity was detected by immunofluorescence microscopy at 4 d posttransfection (Figure 7A). When the filipin intensity in the Rab8 shRNA cells was quantified a significant increase compared with scramble shRNA cells was recorded (Figure 7, B and D). Introduction of the scramble shRNA did not alter filipin intensity in comparison with nontransfected cells (data not shown). The bulk of the filipin deposition in Rab8-depleted cells was localized perinuclearly, with substantial colocalization with Lamp1 (Figure 7C). Indeed, quantification revealed a significant increase in the filipin intensity of Lamp1-positive organelles in Rab8-depleted cells (Figure 7E).

ABCA1 mediates the release of cellular free cholesterol and phospholipids to apoA-I (Oram and Heinecke, 2005) and is transcriptionally activated by LXR. LXR agonists promote cholesterol efflux and represent a promising pharmacological strat-

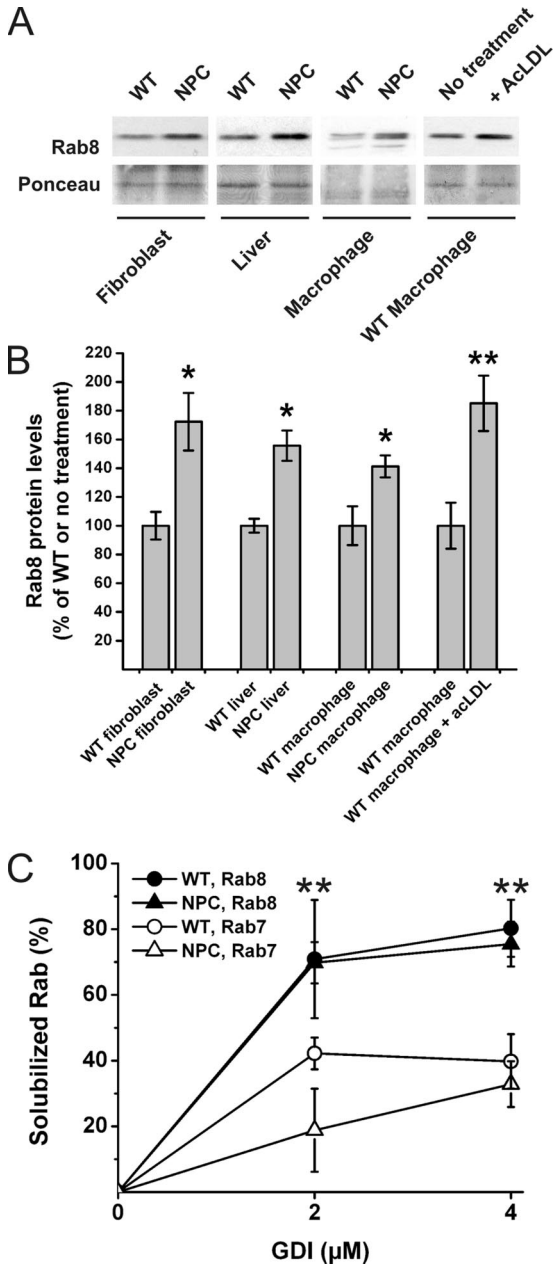

Figure 6. Rab8 is up-regulated and its membrane extractability is not compromised by severe cholesterol deposition. (A) Western blots of 15 μg of protein from cell or tissue lysates as indicated. Filters were Ponceau stained to control for equal loading. (B) Quantification of Western blots (n = 4–6 for each group, mean ± SEM, *p < 0.05, **p ≤ 0.01). (C) Cellular membranes were isolated from control (WT) and F92-116 (NPC) fibroblasts and membranes extracted with increasing amounts of Rab-GDI. The fraction of Rab protein remaining in the membranes was determined by Western blotting with anti-Rab8 antibodies. The same filters were reprobed with anti-Rab7 antibodies (mean ± SD, n = 2–3 for each GDI concentration from at least two independent experiments). **p <0.01 between Rab7 and Rab8 extractability in NPC cells.

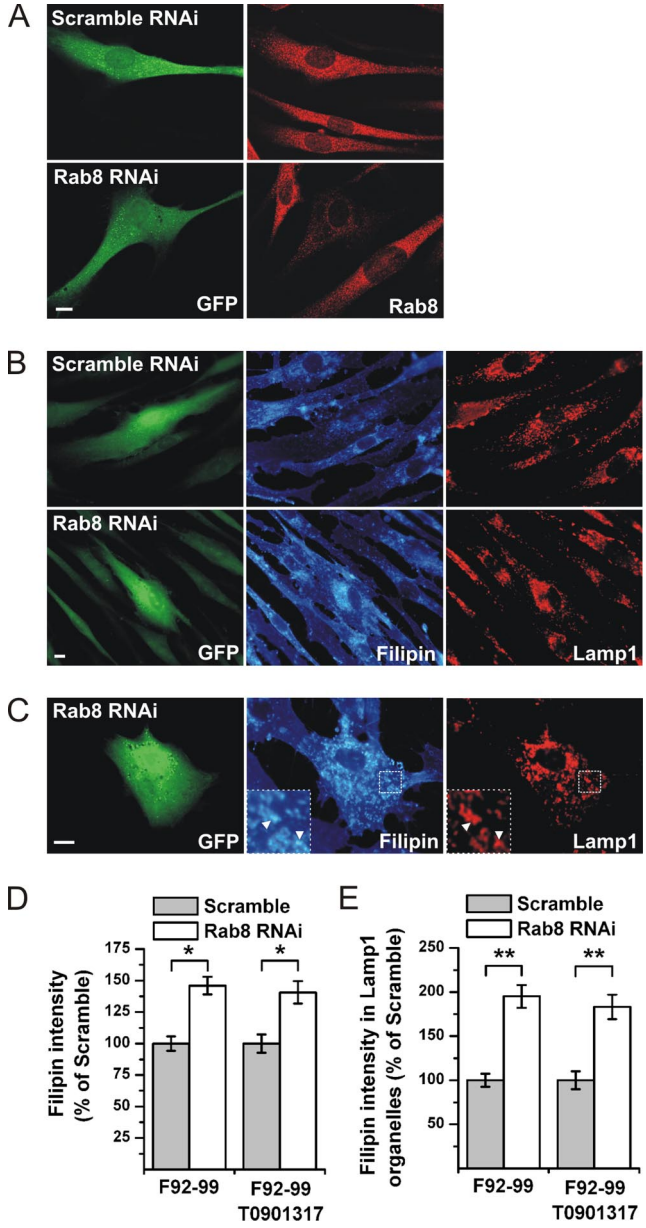

Figure 7. Depletion of Rab8 from fibroblasts results in cellular cholesterol storage. Rab8 was depleted from F92-99 control fibroblasts using RNAi. Cells were transfected with plasmids encoding Rab8 or scramble (control) shRNA, and soluble GFP to identify transfected cells. (A) Decreased Rab8 expression specifically in Rab8 RNAi cells as visualized by anti-Rab8 antibody staining. (B) Rab8 knockdown induces cholesterol accumulation in fibroblasts under normal cell culture conditions, as determined by increased filipin staining intensity. (C) Rab8 shRNA transfected cells show cholesterol accumulation in Lamp1-positive organelles. Quantification of filipin intensity in Rab8 and scramble shRNA-transfected cells (D) and in Lamp1-positive organelles (E; mean ± SEM, n = 50). Where indicated, shRNA-transfected F92-99 fibroblasts were incubated in the presence of 2.5 μM T0901317 for 4 d before fixation and filipin and Lamp1 staining (mean ± SEM, n = 40). *p < 0.05, **p ≤ 0.01. Bars, 10 μm.

egy for cholesterol reduction (Zelcer and Tontonoz, 2006). To study whether an LXR agonist could bypass the cholesterol deposition in Rab8-depleted cells, the Rab8- and scramble shRNA-transfected cells were incubated in the presence of T0901317, and cholesterol levels were assessed by filipin staining. We found that although T0901317 decreased the filipin intensity in both conditions by ~50%, the relative difference between Rab8 and scramble shRNA cells was maintained (Figure 7, D and E). This suggests that the LXR agonist cannot bypass the cholesterol trafficking block induced by Rab8 depletion.

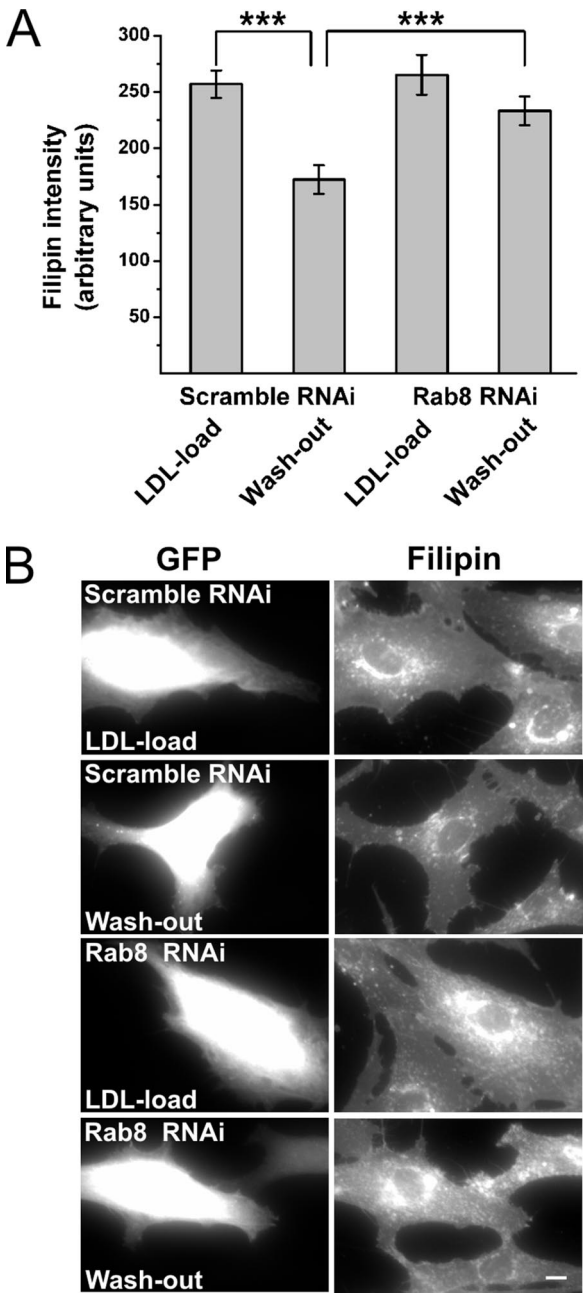

Figure 8. Depletion of Rab8 from fibroblasts retards the clearance of LDL-cholesterol to physiological acceptors. (A) RNAi transfected F92-99 cells were incubated in 10% LPDS for 48 h followed by LDL loading (50 μg protein/ml) for 24 h. One set of coverslips (scramble and Rab8) was fixed at the end of the LDL load, and the rest were incubated in serum-free medium supplemented with 10 μg/ml apoA-I and 0.2% BSA 18 h and then fixed (washout). In contrast to scramble shRNA-transfected cells, Rab8 shRNA cells failed to efflux cholesterol to extracellular acceptors, as determined by filipin intensity (***$p \leq 0.001$, $n = 50$ for each condition). (B) Wide field images demonstrating the retarded clearance of filipin fluorescence in Rab8-depleted cells. Bar, 10 μm.

Rab8 Depletion Inhibits Clearance of LDL-Cholesterol to ApoA-I

To analyze which cholesterol pool contributes to the endosomal cholesterol deposition in Rab8-depleted cells, we incubated the Rab8- or scramble-shRNA transfected cells in lipoprotein-deficient serum for 2 d followed by a 24-h incubation in the presence of LDL and an additional 18 h in the presence of apoA-I. Cells were fixed and filipin stained either immediately after the delipidation, after LDL loading, or after lipid efflux to apoA-I. Quantification of filipin intensity indicated similar cholesterol levels in control and Rab8 knockdown cells after delipidation (data not shown) and LDL loading (Figure 8, A and B), suggesting no difference in the efficiency of LDL-cholesterol uptake or hydrolysis upon Rab8 depletion. However, after cholesterol efflux to apoA-I, filipin intensity was significantly reduced in control cells but not in Rab8 knockdown cells (Figure 8, A and B). This strongly suggests that the removal of LDL-cholesterol from the endocytic circuits becomes slowed down when Rab8 is depleted.

DISCUSSION

In this work, we identified a Rab protein involved in the removal of cholesterol from the endocytic organelles to physiological acceptors. We initially got interested in Rab8 because its overexpression effectively lowered cholesterol accumulation in Niemann–Pick cholesterol-sphingolipidosis cells. Also, the sphingolipid sequestration was alleviated as evidenced by the improved Golgi targeting of CTxB. Two NPC fibroblast lines were used in the study. GM3123 NPC cells exhibited a less prominent cholesterol accumulation phenotype. The heterogeneity of the cholesterol deposition complicates the single cell assessment of Rab complementations in this cell line and may underlie some of the discrepant results obtained previously. We took two approaches to tackle this problem: we used filipin deposition in Lamp1-positive organelles as an alternative method to score cholesterol reduction in late endosomal compartments (Figure 2), and we confirmed the Rab8-induced changes in cholesterol balance with biochemical experiments (Figure 5). GM3123 cells grow faster and are more easily transfected than F92-116 NPC fibroblasts, and they are therefore more amenable for experimentation (our unpublished data). In contrast, the more uniform cholesterol accumulation in F92-116 fibroblasts underwent a more evident reduction upon Rab8 overexpression in spite of the low transfection frequencies (Figure 3).

To probe whether Rab8 is normally involved in cholesterol export from late endosomes, we used RNAi to deplete Rab8 from primary fibroblasts and analyzed the cholesterol levels and localization by filipin staining. We found that Rab8 depletion caused a marked accumulation of cholesterol in normal cells (Figure 7). This accumulation localized to Lamp1-positive organelles, indicating that the Rab8-regulated pathway represents a significant route for cholesterol egress from the endosomal circuits in normal fibroblasts. Importantly, Rab8 overexpression reduced and its depletion induced cholesterol accumulation in late compartments of the endocytic pathway without Rab8 itself localizing to these structures. These observations are relevant for understanding the generation and maintenance of the lysosomal cholesterol storage phenotype: A block in membrane recycling or exocytic/Golgi transport (Rab8 RNAi) can result in lysosomal cholesterol accumulation. Vice versa, the terminal "sink" of cholesterol and sphingolipids characteristic to several sphingolipidoses can be relieved indirectly, possibly by preventing the shunting of more lipids to the traffic jam and decreasing the influx to the lysosome-related organelles. Such a strategy might be more effective than mobilizing cargo within or toward the late endosomal system, as in the case of Rab7 (Figure 3).

The fact that Rab8 does not localize to the cholesterol storing late endosomal and lysosomal organelles may at least partially account for its efficient extractability from NPC membranes by GDI. Recent data indicate that cholesterol interferes directly with the ability of GDI to retrieve Rab proteins from the membrane (Ganley and Pfeffer, 2006). We do not expect Rab8 to function differently from other Rabs in this respect. Rather, the membranes to which Rab8 is targeted are probably less cholesterol-enriched than the late endosomes of NPC cells. Notably, in the same cells, Rab7 resisted GDI extraction, confirming previous findings (Lebrand *et al*., 2002). The differential GDI extractability of Rabs could have implications for directing endosomal membrane transport: Rab proteins that retain functionality during endosomal cholesterol loading may direct membrane transport to some routes at the expense of others.

Several complementary lines of evidence point to the involvement of Rab8 in the process that leads to cholesterol egress from endolysosomes to apoA-I. First, in parallel with the reduction of cholesterol from NPC late endocytic organelles, we observed sterol redistribution to the cell periphery, apparently to the plasma membrane or its immediate vicinity. Second, biochemical data indicated that the cholesterol reduction in NPC cells upon Rab8 overexpression was accompanied by increased cholesterol efflux to apoA-I, whereas cholesterol esterification decreased. This is reminiscent of the LXR activation induced increase in cholesterol efflux at the expense of esterification (Rigamonti *et al*., 2005) and suggests a common route of cholesterol mobilization. Third, Rab8 protein levels increased upon cholesterol loading in cells/tissues that use ABCA1/apoA-I–dependent cholesterol efflux, such as liver and macrophages (Aiello *et al*., 2002; Timmins *et al*., 2005). This was true not only for NPC but also for normal cells, indicating that Rab8 upregulation is not merely a compensatory change in the absence of functional NPC1 but a physiological response in cholesterol challenged cells. Fourth, the endolysosomal cholesterol accumulation of Rab8 depleted control fibroblasts seemed to derive mainly from LDL that was not efficiently cleared from cells by apoA-I. Finally, a potent LXR agonist could not prevent cholesterol deposition in Rab8-depleted cells. This together with the observation that sterol removal to apoA-I was compromised upon Rab8 reduction, strongly suggests that in normal fibroblasts, the ABCA1-dependent cholesterol efflux pathway to apoA-I involves Rab8 function.

How could Rab8 promote cholesterol removal from the endosomal circuits? We envisage that Rab8 may stimulate membrane transport from sterol-enriched endosomal compartments and that this activity may be particularly crucial to prevent sterol sequestration upon LDL-cholesterol hydrolysis. This may involve cholesterol recycling from prelysosomal organelles. The enzyme hydrolyzing the cholesteryl esters in LDL, acid lipase, partially localizes to a prelysosomal compartment (Sugii *et al*., 2003), and the endocytic recycling compartment has been shown to be sterol-enriched (Hao *et al*., 2002). Moreover, when cells were incubated with fluorescent sterol (dehydroergosterol) ester incorporated into LDL, the fluorescent sterol reached the endosomal recycling compartment (Wustner *et al*., 2005). Sterol trafficking from the endosomal recycling system involves membrane transport (Hao *et al*., 2002; Holtta-Vuori *et al*., 2002). A dominant-negative mutant form of Rme1/EHD1, a protein involved in endocytic recycling, causes prominent dehydroergosterol accumulation in the endocytic recycling compartment (Hao *et al*., 2002). Remarkably, our recent data suggest that EHD1 interacts with Rab8 (Peränen and Furuhjelm, unpublished data), providing a direct link between our findings and the previous observations on dehydroergosterol trafficking.

Other possibilities, not exclusive with the idea of Rab8-stimulated sterol recycling, is that Rab8 facilitates the trafficking of ABCA1 and/or apoA-I. A fraction of ABCA1 has been localized to the Golgi (Orso *et al*., 2000) and late endosomes, and endocytic circuits have been implicated in ABCA1-dependent lipid efflux to apoA-I (Neufeld *et al*., 2004; Smith *et al*., 2004; Chen *et al*., 2005). Rab8 also plays a role in cell polarization through reorganization of actin and microtubules (Peranen *et al*., 1996) and may thereby prime the cytoskeletal organization to facilitate cholesterol efflux. Importantly, Cdc42 that regulates the polymerization of actin to form peripheral filopodial protrusions at the leading edge, also interacts with ABCA1 and can be activated by apoA-I (Nofer *et al*., 2006). Collectively, our findings with previous observations pinpoint Rab8 as a key regulatory switch for coordinating the cytoskeletal changes and membrane dynamics in cholesterol efflux.

In conclusion, by taking advantage of a human genetic disease block (lack of functional NPC1) and an induced block of membrane transport (reduction in Rab8 levels), we identified the first Rab protein involved in ABCA1-apoA-I–dependent cholesterol removal from endosomal compartments. The evidence suggests that Rab8 is involved in directing cholesterol to a recycling route that leads the sterol toward the leading edge and promotes its delivery to physiological extracellular acceptors.

ACKNOWLEDGMENTS

We thank Anna Uro and Birgitta Rantala for expert technical assistance. This study was supported by grants from the Academy of Finland, Sigrid Juselius Foundation, Finska Läkaresällskapet, Oskar Öflunds Stiftelse, Sydäntutkimussäätiö, and Helsinki Biomedical Graduate School.

REFERENCES

Aiello, R. J., Brees, D., Bourassa, P. A., Royer, L., Lindsey, S., Coskran, T., Haghpassand, M., and Francone, O. L. (2002). Increased atherosclerosis in hyperlipidemic mice with inactivation of ABCA1 in macrophages. Arterioscler Thromb. Vasc. Biol. *22*, 630–637.

Ang, A. L., Taguchi, T., Francis, S., Folsch, H., Murrells, L. J., Pypaert, M., Warren, G., and Mellman, I. (2004). Recycling endosomes can serve as intermediates during transport from the Golgi to the plasma membrane of MDCK cells. J. Cell Biol. *167*, 531–543.

Bielli, A., Thornqvist, P. O., Hendrick, A. G., Finn, R., Fitzgerald, K., and McCaffrey, M. W. (2001). The small GTPase Rab4A interacts with the central region of cytoplasmic dynein light intermediate chain-1. Biochem. Biophys. Res. Commun. *281*, 1141–1153.

Bligh, E. G., and Dyer, W. J. (1959). A rapid method of total lipid extraction and purification. Can J. Biochem. Physiol. *37*, 911–917.

Blom, T. S., Linder, M. D., Snow, K., Pihko, H., Hess, M. W., Jokitalo, E., Veckman, V., Syvanen, A. C., and Ikonen, E. (2003). Defective endocytic trafficking of NPC1 and NPC2 underlying infantile Niemann-Pick type C disease. Hum. Mol. Genet. *12*, 257–272.

Carstea, E. D., *et al*. (1997). Niemann-Pick C1 disease gene: homology to mediators of cholesterol homeostasis. Science *277*, 228–231.

Cavalli, V., Vilbois, F., Corti, M., Marcote, M. J., Tamura, K., Karin, M., Arkinstall, S., and Gruenberg, J. (2001). The stress-induced MAP kinase p38 regulates endocytic trafficking via the GDI:Rab5 complex. Mol. Cell *7*, 421–432.

Chen, W., Wang, N., and Tall, A. R. (2005). A PEST deletion mutant of ABCA1 shows impaired internalization and defective cholesterol efflux from late endosomes. J. Biol. Chem. *280*, 29277–29281.

Chen, Y. T., Holcomb, C., and Moore, H. P. (1993). Expression and localization of two low molecular weight GTP-binding proteins, Rab8 and Rab10, by epitope tag. Proc. Natl. Acad. Sci. USA *90*, 6508–6512.

Choi, H. Y., Karten, B., Chan, T., Vance, J. E., Greer, W. L., Heidenreich, R. A., Garver, W. S., and Francis, G. A. (2003). Impaired ABCA1-dependent lipid

efflux and hypoalphalipoproteinemia in human Niemann-Pick type C disease. J. Biol. Chem. *278*, 32569–32577.

Choudhury, A., Dominguez, M., Puri, V., Sharma, D. K., Narita, K., Wheatley, C. L., Marks, D. L., and Pagano, R. E. (2002). Rab proteins mediate Golgi transport of caveola-internalized glycosphingolipids and correct lipid trafficking in Niemann-Pick C. cells. J. Clin. Investig. *109*, 1541–1550.

Choudhury, A., Sharma, D. K., Marks, D. L., and Pagano, R. E. (2004). Elevated endosomal cholesterol levels in Niemann-Pick cells inhibit rab4 and perturb membrane recycling. Mol. Biol. Cell *15*, 4500–4511.

Deretic, D., Huber, L. A., Ransom, N., Mancini, M., Simons, K., and Papermaster, D. S. (1995). rab8 in retinal photoreceptors may participate in rhodopsin transport and in rod outer segment disk morphogenesis. J. Cell Sci. *108*, 215–224.

Frolov, A., Zielinski, S. E., Crowley, J. R., Dudley-Rucker, N., Schaffer, J. E., and Ory, D. S. (2003). NPC1 and NPC2 regulate cellular cholesterol homeostasis through generation of low density lipoprotein cholesterol-derived oxysterols. J. Biol. Chem. *278*, 25517–25525.

Gamble, W., Vaughan, M., Kruth, H. S., and Avigan, J. (1978). Procedure for determination of free and total cholesterol in micro- or nanogram amounts suitable for studies with cultured cells. J. Lipid Res. *19*, 1068–1070.

Ganley, I. G., and Pfeffer, S. R. (2006). Cholesterol accumulation sequesters Rab9 and disrupts late endosome function in NPC1-deficient cells. J. Biol. Chem. *281*, 17890–17899.

Goldstein, J. L., Basu, S. K., and Brown, M. S. (1983). Receptor-mediated endocytosis of low-density lipoprotein in cultured cells. Methods Enzymol. *98*, 241–260.

Hao, M., Lin, S. X., Karylowski, O. J., Wustner, D., McGraw, T. E., and Maxfield, F. R. (2002). Vesicular and non-vesicular sterol transport in living cells. The endocytic recycling compartment is a major sterol storage organelle. J. Biol. Chem. *277*, 609–617.

Hattula, K., Furuhjelm, J., Arffman, A., and Peranen, J. (2002). A Rab8-specific GDP/GTP exchange factor is involved in actin remodeling and polarized membrane transport. Mol. Biol. Cell *13*, 3268–3280.

Hattula, K., and Peranen, J. (2000). FIP-2, a coiled-coil protein, links Huntingtin to Rab8 and modulates cellular morphogenesis. Curr. Biol. *10*, 1603–1606.

Holtta-Vuori, M., Maatta, J., Ullrich, O., Kuismanen, E., and Ikonen, E. (2000). Mobilization of late-endosomal cholesterol is inhibited by Rab guanine nucleotide dissociation inhibitor. Curr. Biol. *10*, 95–98.

Holtta-Vuori, M., Tanhuanpaa, K., Mobius, W., Somerharju, P., and Ikonen, E. (2002). Modulation of cellular cholesterol transport and homeostasis by Rab11. Mol. Biol. Cell *13*, 3107–3122.

Huber, L. A., de Hoop, M. J., Dupree, P., Zerial, M., Simons, K., and Dotti, C. (1993a). Protein transport to the dendritic plasma membrane of cultured neurons is regulated by rab8p. J. Cell Biol. *123*, 47–55.

Huber, L. A., Pimplikar, S., Parton, R. G., Virta, H., Zerial, M., and Simons, K. (1993b). Rab8, a small GTPase involved in vesicular traffic between the TGN and the basolateral plasma membrane. J. Cell Biol. *123*, 35–45.

Lebrand, C., Corti, M., Goodson, H., Cosson, P., Cavalli, V., Mayran, N., Faure, J., and Gruenberg, J. (2002). Late endosome motility depends on lipids via the small GTPase Rab7. EMBO J. *21*, 1289–1300.

Liljestrom, P., and Garoff, H. (1991). A new generation of animal cell expression vectors based on the Semliki Forest virus replicon. Biotechnology *9*, 1356–1361.

Liscum, L. (2000). Niemann-Pick type C mutations cause lipid traffic jam. Traffic *1*, 218–225.

Liscum, L., and Faust, J. R. (1987). Low density lipoprotein (LDL)-mediated suppression of cholesterol synthesis and LDL uptake is defective in Niemann-Pick type C fibroblasts. J. Biol. Chem. *262*, 17002–17008.

Lowry, O. H., Rosebrough, N. J., Farr, A. L., and Randall, R. J. (1951). Protein measurement with the Folin phenol reagent. J. Biol. Chem. *193*, 265–275.

Naureckiene, S., Sleat, D. E., Lackland, H., Fensom, A., Vanier, M. T., Wattiaux, R., Jadot, M., and Lobel, P. (2000). Identification of HE1 as the second gene of Niemann-Pick C disease. Science *290*, 2298–2301.

Neufeld, E. B., *et al*. (2004). The ABCA1 transporter modulates late endocytic trafficking: insights from the correction of the genetic defect in Tangier disease. J. Biol. Chem. *279*, 15571–15578.

Nofer, J. R., Remaley, A. T., Feuerborn, R., Wolinnska, I., Engel, T., von Eckardstein, A., and Assmann, G. (2006). Apolipoprotein A-I activates Cdc42 signaling through the ABCA1 transporter. J. Lipid Res. *47*, 794–803.

Ohgami, N., Ko, D. C., Thomas, M., Scott, M. P., Chang, C. C., and Chang, T. Y. (2004). Binding between the Niemann-Pick C1 protein and a photoactivatable cholesterol analog requires a functional sterol-sensing domain. Proc. Natl. Acad. Sci. USA *101*, 12473–12478.

Okamura, N., Kiuchi, S., Tamba, M., Kashima, T., Hiramoto, S., Baba, T., Dacheux, F., Dacheux, J. L., Sugita, Y., and Jin, Y. Z. (1999). A porcine homolog of the major secretory protein of human epididymis, HE1, specifically binds cholesterol. Biochim. Biophys. Acta *1438*, 377–387.

Olkkonen, V. M., Liljestrom, P., Garoff, H., Simons, K., and Dotti, C. G. (1993). Expression of heterologous proteins in cultured rat hippocampal neurons using the Semliki Forest virus vector. J. Neurosci. Res. *35*, 445–451.

Oram, J. F., and Heinecke, J. W. (2005). ATP-binding cassette transporter A *1*, a cell cholesterol exporter that protects against cardiovascular disease. Physiol. Rev. *85*, 1343–1372.

Orso, E., *et al*. (2000). Transport of lipids from Golgi to plasma membrane is defective in tangier disease patients and Abc1-deficient mice. Nat. Genet. *24*, 192–196.

Pentchev, P. G., Brady, R. O., Blanchette-Mackie, E. J., Vanier, M. T., Carstea, E. D., Parker, C. C., Goldin, E., and Roff, C. F. (1994). The Niemann-Pick C lesion and its relationship to the intracellular distribution and utilization of LDL cholesterol. Biochim. Biophys. Acta *1225*, 235–243.

Pentchev, P. G., Comly, M. E., Kruth, H. S., Vanier, M. T., Wenger, D. A., Patel, S., and Brady, R. O. (1985). A defect in cholesterol esterification in Niemann-Pick disease (type C) patients. Proc. Natl. Acad. Sci. USA *82*, 8247–8251.

Peranen, J., Auvinen, P., Virta, H., Wepf, R., and Simons, K. (1996). Rab8 promotes polarized membrane transport through reorganization of actin and microtubules in fibroblasts. J. Cell Biol. *135*, 153–167.

Rigamonti, E., *et al*. (2005). Liver X receptor activation controls intracellular cholesterol trafficking and esterification in human macrophages. Circ. Res. *97*, 682–689.

Schuck, S., Manninen, A., Honsho, M., Fullekrug, J., and Simons, K. (2004). Generation of single and double knockdowns in polarized epithelial cells by retrovirus-mediated RNA interference. Proc. Natl. Acad. Sci. USA *101*, 4912–4917.

Simons, K., and Gruenberg, J. (2000). Jamming the endosomal system: lipid rafts and lysosomal storage diseases. Trends Cell Biol. *10*, 459–462.

Smith, J. D., Le Goff, W., Settle, M., Brubaker, G., Waelde, C., Horwitz, A., and Oda, M. N. (2004). ABCA1 mediates concurrent cholesterol and phospholipid efflux to apolipoprotein A-I. J Lipid Res. *45*, 635–644.

Sugii, S., Reid, P. C., Ohgami, N., Du, H., and Chang, T. Y. (2003). Distinct endosomal compartments in early trafficking of low density lipoprotein-derived cholesterol. J. Biol. Chem. *278*, 27180–27189.

Sugimoto, Y., Ninomiya, H., Ohsaki, Y., Higaki, K., Davies, J. P., Ioannou, Y. A., and Ohno, K. (2001). Accumulation of cholera toxin and GM1 ganglioside in the early endosome of Niemann-Pick C1-deficient cells. Proc. Natl. Acad. Sci. USA *98*, 12391–12396.

Timmins, J. M., *et al*. (2005). Targeted inactivation of hepatic Abca1 causes profound hypoalphalipoproteinemia and kidney hypercatabolism of apoA–I. J. Clin. Invest. *115*, 1333–1342.

Walter, M., Davies, J. P., and Ioannou, Y. A. (2003). Telomerase immortalization upregulates Rab9 expression and restores LDL cholesterol egress from Niemann-Pick C1 late endosomes. J. Lipid Res. *44*, 243–253.

van der Sluijs, P., Hull, M., Huber, L. A., Male, P., Goud, B., and Mellman, I. (1992). Reversible phosphorylation–dephosphorylation determines the localization of rab4 during the cell cycle. EMBO J. *11*, 4379–4389.

Wustner, D., Mondal, M., Tabas, I., and Maxfield, F. R. (2005). Direct observation of rapid internalization and intracellular transport of sterol by macrophage foam cells. Traffic *6*, 396–412.

Zelcer, N., and Tontonoz, P. (2006). Liver X receptors as integrators of metabolic and inflammatory signaling. J. Clin. Investig. *116*, 607–614.

Zerial, M., and McBride, H. (2001). Rab proteins as membrane organizers. Nat. Rev. Mol. Cell Biol. *2*, 107–117.